ORIGINAL RESEARCH

miR-493-5p Silenced by DNA Methylation Promotes Angiogenesis via Exosomes and VEGF-A-Mediated Intracellular Cross-Talk Between ESCC Cells and HUVECs

Zhaohua Xiao[1,]*, Jiangfeng Zhao[1,]*, Guanhong Ji[1], Xiangqing Song[1], Xia Xue[2], Wenhao Zhang[1], Guomeng Sha[1], Yongjia Zhou[1], Jie Zhou[1], Zhongxian Tian[1,3], Xiaogang Zhao[1,3], Ning Jiang[1]

[1]Department of Thoracic Surgery, the Second Hospital of Shandong University, Jinan, 250033, People's Republic of China; [2]Department of Pharmacy, the Second Hospital of Shandong University, Jinan, People's Republic of China; [3]Key Laboratory of Chest Cancer, Shandong University, the Second Hospital of Shandong University, Jinan, People's Republic of China

*These authors contributed equally to this work

Correspondence: Ning Jiang, Department of Thoracic Surgery, the Second Hospital of Shandong University, Jinan, 250033, People's Republic of China, Tel +86-17660081908, Email sdujiangning@163.com

Background: Exosomal microRNAs (miRNAs) in the tumor microenvironment play crucial roles in tumorigenesis and tumor progression by participating in intercellular cross-talk. However, the functions of exosomal miRNAs and the mechanisms by which they regulate esophageal squamous cell carcinoma (ESCC) progression are unclear.

Methods: RNA sequencing and GEO analysis were conducted to identify candidate exosomal miRNAs involved in ESCC development. Receiver operating characteristic curve analysis was performed to assess the diagnostic value of plasma exosomal miR-493-5p. EdU, tube formation and Transwell assays were used to investigate the effects of exosomal miR-493-5p on human umbilical vein endothelial cells (HUVECs). A subcutaneous xenograft model was used to evaluate the antitumor effects of miR-493-5p and decitabine (a DNA methyltransferase inhibitor). The relationship between miR-493-5p and SP1/SP3 was revealed via a dual-luciferase reporter assay. A series of rescue assays were subsequently performed to investigate whether SP1/SP3 participate in exosomal miR-493-5p-mediated ESCC angiogenesis.

Results: We found that miR-493-5p expression was notably reduced in the plasma exosomes of ESCC patients, which showed the high potential value in early ESCC diagnosis. Additionally, miR-493-5p, as a candidate tumor suppressor, inhibited the proliferation, migration and tube formation of HUVECs by suppressing the expression of VEGFA and exerted its angiostatic effect via exosomes. Moreover, we found that SP1/SP3 are direct targets of miR-493-5p and that re-expression of SP1/SP3 could reverse the inhibitory effects of miR-493-5p. Further investigation revealed that miR-493-5p expression could be regulated by DNA methyltransferase 3A (DNMT3A) and DNMT3B, and either miR-493-5p overexpression or restoration of miR-493-5p expression with decitabine increased the antitumor effects of bevacizumab.

Conclusion: Exosomal miR-493-5p is a highly valuable ESCC diagnosis marker and inhibits ESCC-associated angiogenesis. miR-493-5p can be silenced via DNA methylation, and restoration of miR-493-5p expression with decitabine increases the antitumor effects of bevacizumab, suggesting its potential as a therapeutic target for ESCC treatment.

Keywords: esophageal squamous cell carcinoma, exosomes, miR-493-5p, VEGFA, angiogenesis

Introduction

Esophageal cancer (EC), the seventh most common and sixth most deadly cancer worldwide, is a key threat to human health.[1] There were approximately 0.6 million newly diagnosed cases worldwide in 2022, more than half of which were found in China, and esophageal squamous cell carcinoma (ESCC) accounts for 85% of the cases.[2] The prognosis of

ESCC is poor, with a five-year survival rate less than 20%.[3] Although there has been great progress in recent years for diagnostic methods, the early symptoms of ESCC are still too subtle to be noticed, so most ESCC cases are first diagnosed in the advanced stage.[4] Because there is currently no reliable targeted therapy for ESCC, patients generally have fewer options for treatment.[5] Elucidating the underlying mechanism of ESCC development and identifying valuable biomarker targets for diagnosis or treatment are highly important for improving ESCC prognosis.

Exosomes are extracellular vesicles ranging in size from 30–150 nm that exist in various body fluids.[6] It has been reported that cancer cells secrete different exosomal components than normal cells, and these components include distinct proteins, lipids and nucleic acids [such as microRNAs (miRNAs) and long noncoding RNAs].[7] Thus, exosomes, which can be obtained by liquid biopsy, have been widely investigated as biomarkers for early diagnosis, prognosis prediction and recurrence monitoring in cancer patients.[8,9] Moreover, exosomes can transport molecular signals from host cells. Accumulating evidence suggests that cancer-derived exosomes remodel the local tumor microenvironment by altering intercellular communication, which regulates angiogenesis, lymphangiogenesis, tumor immunity, metastasis and drug resistance in tumors.[10,11] Recently, the clinical potential and function of exosomes in ESCC have been gradually revealed,[12,13] exosomes-based therapy shows bright perspectives in ESCC treatment. Through RNA sequencing, we found a close relationship between plasma exosomal miR-493-5p levels and the progression of ESCC. However, whether exosomal miR-493-5p can be treated as a noninvasive biomarker for early detection of ESCC and how miR-493-5p regulates ESCC occurrence and development are unclear and need further investigation.

Angiogenesis, the formation of new blood vessels from preexisting vessels, is a critical mechanism for tumor development. During tumor growth, oxygen and nutrients in the tumor environment are depleted, leading to hypoxia, which results in the formation of new blood vessels to obtain additional oxygen and nutrients.[14] The abnormal and rapid formation of tumor blood vessels is regulated by an imbalance in proangiogenic and antiangiogenic factors. Vascular endothelial growth factors (VEGFs), especially VEGFA, are recognized as some of the most powerful proangiogenic factors. By binding to its specific receptors VEGFR1 and VEGFR2, VEGFA can activate distinct signaling pathways and expand the tumor vascular bed.[15] The United States Food and Drug Administration (FDA) has approved several anti-VEGFA agents, such as bevacizumab, to suppress angiogenesis in many malignancies, and these agents have great effects.[16,17] However, the effects are limited in ESCC for several reasons, especially the existence of VEGFA-independent pathway.[18] Therefore, exploring the mechanism of the VEGFA-independent pathway and further customizing combined treatment regimens are highly important for treating ESCC. Recently, exosomal miRNAs have been recognized as key mediators of tumor angiogenesis.[19–21] However, the roles and regulatory mechanisms of exosomal miR-493-5p in ESCC angiogenesis have not been fully elucidated and warrant further investigation.

In this study, we found that miR-493-5p expression was notably reduced in the plasma exosomes of ESCC patients vs those of healthy controls, and plasma exosomal miR-493-5p had high diagnostic value for ESCC. In addition, we found that miR-493-5p inhibited the proliferation, migration, and tube formation of HUVECs in a VEGFA-dependent manner and exerted an angiostatic effect via exosomes. Overexpression of miR-493-5p or restoration of miR-493-5p expression with decitabine could increase the antitumor effects of bevacizumab. These findings provide us with a new noninvasive biomarker for ESCC diagnosis and indicate a potential therapeutic strategy for ESCC treatment.

Material and Methods
Clinical Samples
Fifty-eight ESCC patients who underwent radical surgery at the Second Hospital of Shandong University (Jinan, China) between May 2020 and October 2021 were enrolled in this study. None of the patients received any anticancer treatments before biopsy collection. We collected peripheral blood from these 58 ESCC patients preoperatively and used peripheral blood from 30 healthy volunteers as controls. Surgical tissues were collected from 36 of the 58 ESCC patients during surgery and immediately placed in liquid nitrogen.

RNA Sequencing and Bioinformatics Analysis

RNA sequencing was performed by Novogene (Beijing, China) using plasma exosomes from 5 ESCC patients with lymph node metastasis (LN$^+$) and 5 ESCC patients without LN metastasis (LN$^-$) as we previously described.[22] Firstly, 3 μg of RNA was used to generate a small RNA library, and sequenced on an Illumina HiSeq 2500/2000 platform. Then, DESeq R package (3.0.3) was used for differential expression analysis. $P<0.05$ and log$_2$|fold change| > 1 were set as the thresholds for significant differential expression. The raw data have been uploaded in the Gene Expression Omnibus (GEO) database (GEO number: GSE214259). The GEO dataset GSE155360 contains data from serum exosomes of 20 ESCC patients with or without LN metastasis was employed to analyze differentially expressed genes by the "limma" package. Log$_2$|fold change| > 1 was set as the screening threshold. The miRDB, miRDIP, ENCORI and TargetScan databases were used to predicted the targeted genes of miR-493-5p.

Cell Culture and Transfection

All cell lines used in this study were purchased from Fu Heng Biological (Shanghai, China). Eca109 and KYSE150 cells were cultured in RPMI-1640 medium (Corning Cellgro, Manassas, VA, USA) supplemented with 10% fetal bovine serum (FBS; HyClone, Logan, UT, USA). HEEC, HET-1A and HEK293T cells were cultured in DMEM (Corning) supplemented with 10% FBS. HUVECs were maintained in endothelial cell medium (ECM; ScienCell) supplemented with 5% FBS and 1% endothelial growth medium. All cells were cultured at 37°C in a 5% CO$_2$ humidified incubator.

The miR-493-5p and DNMT1 overexpression lentivirus plasmids were synthesized by TSINGKE Biological Technology (Beijing, China). The SP1, SP3, DNMT3A and DNMT3B overexpression lentivirus plasmids were purchased from Miaoling Biology (Wuhan, China). The miR-493-5p mimic and inhibitor were purchased from GenePharma Co., Ltd. (Shanghai, China) and were transduced into HEK293T cells or HUVECs by Lipofectamine^{TM} 3000 (Invitrogen, Carlsbad, CA, USA). The sequences of the miR-493-5p mimic and inhibitor are listed in Supplementary Table 1. SiRNAs against SP1 and SP3 and shRNAs against DNMT1, DNMT3A, and DNMT3B synthesized by TSINGKE were transduced into Eca109 cells or HUVECs through siTran 2.0 siRNA transfection reagent (Origene). The siRNA and shRNA sequences are shown in Supplementary Table 2. Decitabine and bevacizumab were purchased from MedChemExpress (Shanghai, China).

Isolation and Identification of Exosomes

The cell culture medium (CM) was centrifuged at 2000 ×g for 10 min and 10,000 ×g for 30 min, and the precipitate was removed. The supernatant was then ultracentrifuged at 110,000 ×g for 70 min to collect the exosomes using an Optima XPN-80 Ultracentrifuge (Beckman Coulter, California, USA). Plasma exosomes were extracted via an exosome isolation kit (System Biosciences) according to the manufacturer's instructions. Finally, the exosome precipitate was resuspended in PBS and stored in a −80°C freezer.

To ensure that the exosomes were separated successfully, we used transmission electron microscopy (TEM; Thermo Scientific, Carlsbad, CA, USA) to observe the morphology of the exosomes. NanoSight tracking analysis (NTA, NanoSight NS300, Malvern, UK) was used to assess the size distribution of the exosomes. Finally, we performed Western blotting with the exosome-specific protein markers CD63 and TSG101 and the negative marker GRP94.

Exosome Labeling and Uptake Assays

The purified exosomes were labeled with a PKH67 green fluorescence labeling kit (Sigma–Aldrich, MO, USA). Then, the labeled exosomes were cocultured with HUVECs. A confocal microscope (Zeiss, Germany) was used to observe the cells, which were stained with 4.6-diamidino-2-phenylindole (DAPI; Solarbio, Beijing, China).

Quantitative Real-Time PCR (qRT–PCR)

Total RNA from exosomes, tissues and cells was extracted with the miRcute miRNA Isolation Kit (Tiangen Biotech, Beijing, China) and reverse-transcribed into cDNA using the miRNA First-Strand cDNA Synthesis Kit and the lnRcute lncRNA First-Strand cDNA Synthesis Kit (Tiangen). qRT–PCR was conducted using a QuantStudio^{TM} 5 Real-Time PCR System (Thermo Scientific). β-Actin and U6 snRNA were chosen as internal controls. The 2$^{-\Delta\Delta CT}$ analytical method was

used to calculate the relative expression levels. The primers used in this study were synthesized by TSINGKE and are listed in Supplementary Table 3.

Western Blotting

Cells were harvested and lysed with RIPA lysis buffer (Beyotime, China). Proteins were separated by 8–12% SDS–PAGE and transferred to PVDF membranes (Millipore). The membranes were subsequently blocked in 5% skim milk for 1 h and incubated with the corresponding primary antibodies at 4°C overnight. The next day, the membranes were washed three times with TBST and incubated with secondary antibodies for 1 h. After washing three times with TBST, the membranes were visualized with an enhanced chemiluminescence (ECL) system. GAPDH or β-Actin served as the internal control, and the primary antibodies used in this study are shown in Supplementary Table 4.

Enzyme-Linked Immunosorbent Assay (ELISA)

After transfection for 48 h, the cell culture medium was collected and centrifuged at $1000 \times g$ for 20 min at 4°C. The VEGFA concentration in the supernatant was subsequently measured via a VEGFA ELISA Kit (Elabscience, Wuhan, China) according to the manufacturer's instructions. Finally, the optical density (OD) at 450 nm was measured by a multifunctional enzyme-linked analyzer (BioTek, USA).

Immunohistochemistry (IHC)

Four-millimeter-thick section slides were stained with antibodies against CD31 and VEGFA with an IHC kit (Zsbio, Beijing, China). After incubation with primary and secondary antibodies, chromogenic reactions were revealed by 3.3′-diaminobenzidine tetrahydrochloride hydrate (DAB) staining. Images were captured with a NanoZoomer Digital Pathology scanner (HAMAMATSU, Japan). The results were evaluated according to the mean integrated optical density (IOD) via ImageJ software. The primary antibodies used in the IHC analysis are also shown in Supplementary Table 4.

5-Ethynyl-2'-Deoxyuridine (EdU) Assay

A total of 3×10^3 cells were seeded in 96-well plates and incubated for 24 h. After incubation with 100 μL of EdU solution (Beyotime) and fixation with 4% paraformaldehyde, the cells were washed with 3% bovine serum albumin (BSA) and permeabilized with 0.5% Triton X-100. Finally, 1× Hoechst 33342 reaction solution was used to stain the nuclei, and images were captured using a fluorescence microscope. The percentage of EdU-positive cells was calculated as follows: (number of EdU-stained cells/number of Hoechst-stained cells) × 100%. The experiment was performed three times.

Wound Healing Assay

A total of 4×10^4 cells were added to each well with a culture insert (Ibidi, Germany) and incubated overnight, and the insert was removed when the cells reached 100% confluency. After washing with 1×PBS, the cells were cultured in serum-free medium. Images were captured by an inverted microscope every 12 h. The wound healing rate was analyzed with ImageJ software. The experiment was performed three times.

Transwell Assay

In the invasion assay, 50 μL of Matrigel (1:10; BD Biosciences, San Jose, CA, USA) was used to precoat the upper membranes of the Transwell chambers (8 μm pore size; Corning); in the migration assay, uncoated Transwell chambers were used. A total of 5×10^4 cells suspended in 200 μL of serum-free medium were seeded in the upper chambers, and 600 μL of medium supplemented with 10% FBS was added to the lower chamber. After culturing for 48 h, the cells that penetrated the lower membranes were stained with hematoxylin and counted. The experiment was performed in triplicate.

Tube Formation Assay

One hundred microlitres of Matrigel (1:1; BD Biosciences) was added to 48-microwell plates, which were subsequently incubated at 37°C for 30 min for solidification. Then, 3×10^4 HUVECs were resuspended in ECM supplemented with the corresponding exosomes and added to the microwells. After incubation for 4–6 h, the capillary-like structures were

observed using an inverted microscope. The length of tubes per field was counted using ImageJ software. The experiment was performed in triplicate.

Dual-Luciferase Reporter Assay

The 3' untranslated regions (UTRs) of SP1 and SP3, which contain binding sites for miR-493-5p or their mutated versions, were cloned and inserted into the pmirGLO vector. HEK293T cells were cotransfected with a wild-type (WT) vector or mutant (MUT) vector and miR-493-5p mimics or mimics-NC using Lipofectamine^{TM} 3000 (Invitrogen). After cotransfection for 48 h, luciferase activity was detected through a dual-luciferase reporter assay kit (Promega, Madison, WI, USA). The firefly luciferase activity was normalized to the Renilla luciferase activity. The experiment was performed in triplicate.

Vivo Xenograft Test

Four-week-old female BALB/c nude mice were purchased from HFK Biotechnology (Beijing, China). To explore the effects of miR-493-5p in sensitizing mice to bevacizumab, the mice were randomly divided into two groups and engrafted with 4×10^6 Eca109-NC or Eca109-miR-493-5p-OE cells in the axilla. Then, each group was intraperitoneally injected with bevacizumab (2.5 mg/kg) or PBS every two days. Xenograft formation in nude mice was monitored and calculated with the following formula: tumor volume $=$ length$\times$width^2/2. Three weeks after the initial implantation, the tumors were harvested, measured and embedded in paraffin for IHC analysis.

To observe the synergistic antitumor effects of decitabine and bevacizumab, 4×10^6 Eca109 cells were injected into the axilla of the mice. After implantation for one week, the mice were randomly divided into 4 groups and intraperitoneally injected with PBS, bevacizumab (2.5 mg/kg), decitabine (1.0 mg/kg), or bevacizumab (2.5 mg/kg) plus decitabine (1.0 mg/kg) every two days. Three weeks after the initial implantation, the tumors were harvested, measured and embedded in paraffin for IHC analysis.

Statistical Analysis

All the data were analyzed using GraphPad Prism 9.0.1 (San Diego, CA, USA). Statistical significance was analyzed via Student's *t* test for comparisons between two groups and one-way analysis of variance (ANOVA) for comparisons among multiple groups. The chi-square test was applied to compare categorical variables. Pearson's correlation coefficient analysis was used to analyze the correlations. All the results are expressed as the mean ± standard deviation (SD), and $P<0.05$ was considered to indicate a significant difference.

Results

Downregulation of Exosomal MiR-493-5p is Associated with Poor Clinicopathological Characteristics in ESCC Patients

To identify the candidate exosomal miRNAs involved in ESCC progression, we isolated plasma exosomes from 5 LN$^+$ ESCC patients and 5 LN$^-$ ESCC patients. After plasma exosomes were characterized by TEM, NTA and Western blotting (Figure 1A–C), RNA sequencing was performed by Novogene (Beijing, China). As shown in Figure 1D, 6 miRNAs were significantly upregulated, and 4 miRNAs were downregulated in the plasma exosomes of LN$^+$ ESCC patients vs LN$^-$ ESCC patients according to cutoff values of log$_2$|fold change|> 1 and $P<0.05$. The raw and processed data were uploaded to the GEO database (GEO number: GSE214259). After combination with the GSE155360 dataset, which includes the miRNA profiles from the serum exosomes of 20 ESCC patients, 2 miRNAs (miR-493-5p and miR-10527-5p) that were differentially expressed in both datasets were identified (Figure 1E).

Since we elucidated the functional roles and mechanisms of exosomal miR-10527-5p previously,[22] in this study, we focused mainly on miR-493-5p, which has been reported to be a tumor suppressor and to be downregulated in various cancers.[23–25] First, qRT–PCR was applied to detect the expression of miR-493-5p in plasma exosome samples from 58 ESCC patients and 30 healthy individuals. As depicted in Figure 1F, the exosomal miR-493-5p level was significantly lower in LN$^+$ ESCC patients (n=38) than in the LN$^-$ patients (n=20), which was consistent with the RNA sequencing
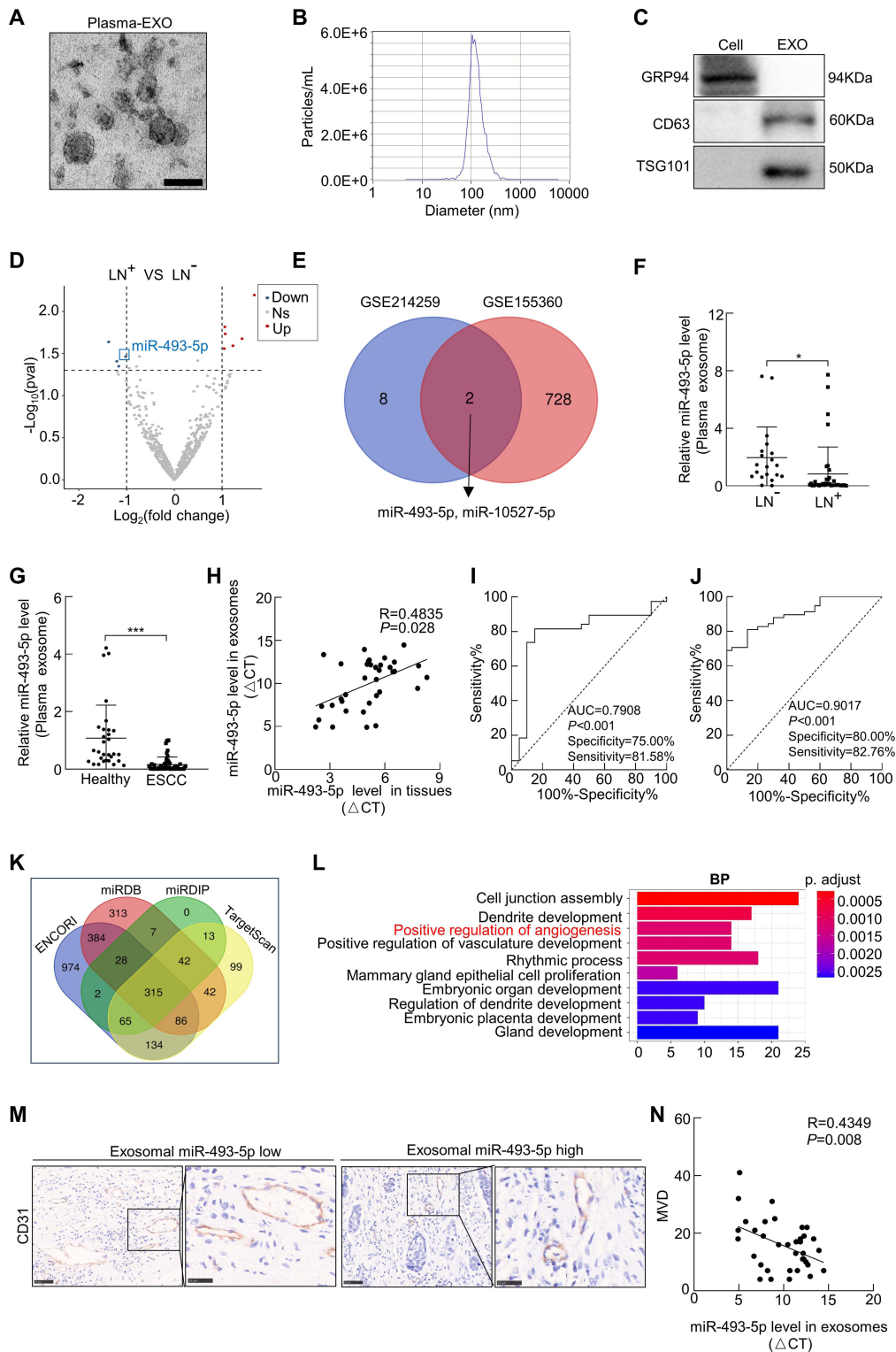
Figure 1 miR-493-5p is reduced in ESCC and functions as an angiostatic factor. (**A** and **B**) The morphology and size distribution of the plasma exosomes (EXO) were identified by a transmission electron microscope (scale bar=100 nm) and NanoSight tracking analysis. (**C**) Western blot analysis of CD63, TSG101, and negative marker GRP94 in exosomes. (**D**) The volcano map indicates differentially expressed miRNAs from RNA sequencing. (**E**) Intersection of differentially expressed miRNAs from our RNA sequencing results (GSE214259) and the GSE155360 dataset. (**F**) qRT–PCR analysis of miR-493-5p relative level in plasma exosomes from 20 LN⁻ ESCC patients and 38 LN⁺ ESCC patients. (**G**) qRT–PCR analysis of miR-493-5p relative level in plasma exosomes from 58 ESCC patients and 30 healthy individuals. (**H**) Correlation between plasma exosomal miR-493-5p expression levels and paired miR-493-5p expression levels in ESCC tissues. (**I** and **J**) ROC curve analysis of plasma exosomal miR-493-5p in predicting LN status and diagnosis of ESCC. (**K**) Venn diagrams represent candidate target genes of miR-493-5p predicted via the miRDB, miRDIP, ENCORI, and TargetScan databases. (**L**) GO analysis of the candidate genes (BP, biological process). (**M**) Representative images of IHC staining for CD31 expression in ESCC tissues. Scale bar, 50 μm (left) and 100 μm (right). (**N**) Correlation between microvessel density (MVD) and paired exosomal miR-493-5p expression levels in ESCC tissues. In vitro experiments were performed in triplicate, and the data are represented as the mean ± SD, *P<0.05, ***P<0.001.

results. Compared with that in ESCC patients, the exosomal miR-493-5p expression level was significantly greater in healthy individuals (Figure 1G). In addition, the results of Pearson analysis revealed that the expression of miR-493-5p in plasma exosomes was positively correlated with that in tissues (Figure 1H). The receiver operating characteristic (ROC) curve analysis showed that the area under the ROC curve (AUC), sensitivity and specificity values of plasma exosomal miR-493-5p in discriminating preoperative LN status were 0.7908, 81.58% and 75.00%, respectively (Figure 1I). Whereas, the AUC, sensitivity and specificity values of plasma exosomal miR-493-5p in ESCC diagnosis were 0.9017, 82.76% and 80.00%, respectively (Figure 1J), which suggested that exosomal miR-493-5p had higher accuracy in ESCC diagnosis than predicting the preoperative LN status. Next, we classified these 58 ESCC patients into 2 groups based on the median exosomal miR-493-5p levels and investigated the association between exosomal miR-493-5p levels and clinicopathological parameters using the chi-square test. As shown in Table 1, exosomal miR-493-5p levels were significantly negatively correlated with T status (P=0.0118), LNM status (P<0.001) and tumor stage (P<0.001), indicating that downregulation of exosomal miR-493-5p is strongly associated with poor clinicopathological characteristics in ESCC patients.

MiR-493-5p Acts as a Tumor Suppressor and an Angiostatic Factor

To further assess the biological functions of miR-493-5p in ESCC cells, we compared the expression levels of miR-493-5p in 2 esophageal epithelial cell lines (HET-1A and HEEC) and 4 ESCC cell lines (KYSE30, Eca109, KYSE150 and EC9706). As shown in Figure S1A, the expression level of miR-493-5p in ESCC cell lines was markedly lower than that in normal esophageal epithelial cell lines. Next, Eca109 and KYSE150 cells were transfected with miR-493-5p over-expression (miR-493-5p OE) lentiviruses and miR-493-5p inhibitor, respectively (Figure S1B). Wound healing and Transwell assays showed that miR-493-5p OE notably suppressed the migration and invasion of ESCC cells and that the miR-493-5p inhibitor significantly promoted these effects (Figure S1C–S1E), confirming that miR-493-5p may serve as a tumor suppressor.

Table 1 Relationship Between Plasma Exosomal miR-493-5p Expression and Clinicopathologic Characteristics in ESCC

Clinicopathologic Characteristics	Cases (n=58)	Exosomal miR-493-5p level		
		Low (n=29)	High (n=29)	*P*-value
Gender				
Male	43	22	21	0.7643
female	15	7	8	
Age (years)				
<60	20	10	10	0.9999
≥60	38	19	19	
Differentiation Degree				
Low	37	21	16	0.1719
Mid-high	21	8	13	
T Stage				
T1-2	19	5	14	0.0118*
T3-4	39	24	15	
LN Status				
N0	20	2	18	<0.001***
N1-3	38	27	11	
Pathologic stage				
I+II	19	2	17	<0.001***
III+IV	39	27	12	

Notes: *P<0.05; ***P<0.001.
Abbreviations: ESCC, esophageal squamous cell carcinoma; T, tumor; LN, lymph node.

To further clarify how exosomal miR-493-5p regulates ESCC progression, we performed Gene Ontology (GO) analysis using 315 miR-493-5p target genes predicted via the miRDB, miRDIP, ENCORI and TargetScan databases (Figure 1K and L). GO enrichment analysis indicated that these genes were enriched in "positive regulation of angiogenesis". Clinically, plasma exosomal miR-493-5p levels were negatively correlated with microvessel density (MVD) in corresponding ESCC tissues (Figure 1M and N). Considering the critical role of angiogenesis in tumor development, we next assessed the antiangiogenic effect of miR-493-5p in vitro. HUVECs were transfected with miR-493-5p mimics and mimics-NC (Figure S2A), and the results of EdU, tube formation, and Transwell assays suggested that miR-493-5p mimics markedly suppressed the proliferation, tube formation and migration of HUVECs (Figure S2B–S2F), indicating that miR-493-5p is an angiostatic factor.

Exosomal miR-493-5p Suppresses the Cell Proliferation, Migration, and Tube Formation of HUVECs in vitro

In the tumor microenvironment, tumor-derived exosomal miRNAs can be absorbed by vascular endothelial cells and regulate their biological behaviors.[19,26] To determine whether miR-493-5p functions by hiding in exosomes, we purified exosomes from the CM of Eca109 cells and characterized them via TEM, NTA and Western blot assays (Figure 2A–C). The qRT–PCR results confirmed that miR-493-5p levels were also markedly lower in ESCC cell-secreted exosomes than in the exosomes secreted from human esophageal epithelial cells (Figure 2D). Additionally, the level of exosomal miR-493-5p was significantly positively correlated with the miR-493-5p content in cells (R=0.9139, P=0.0108; Figure 2E). The qRT–PCR results revealed that miR-493-5p was more highly expressed in exosomes extracted from miR-493-5p-overexpressing cells (miR-493-5p OE-EXOs) than in exosomes extracted from cells transfected with the control vector (Vector-EXOs; Figure 2F). We then cocultured PKH67-labeled exosomes derived from Eca109 cells with HUVECs. Under a confocal microscope, the green fluorescence signal was observed mainly in the perinuclear region of HUVECs (Figure 2G). Moreover, the qRT–PCR results revealed that coculture of Eca109$_{miR-493-5p~OE}$-EXOs obviously increased the level of miR-493-5p in HUVECs in a time-dependent manner (Figure 2H). Collectively, these findings clearly demonstrated that the horizontal transfer of miR-493-5p from ESCC cells to HUVECs can occur through exosomes. To determine whether exogenous miR-493-5p functions identically to endogenous miR-493-5p, we cocultured exosomes from different sources with HUVECs. Figure 2I illustrates that Eca109$_{miR-493-5p~OE}$-EXOs significantly decreased the proliferation, migration and tube formation capacities of HUVECs. However, treatment with Eca109$_{miR-493-5p-inhibitor}$-EXOs had the opposite effect (Figure 2J). Taken together, these results indicated that exosomal miR-493-5p could suppress the angiogenesis ability of HUVECs.

miR-493-5p Increases the Anti-ESCC Effect of Bevacizumab via a VEGFA-Dependent Pathway

Among the various proangiogenic factors, VEGFA is recognized as one of the most powerful regulators of blood vessel formation. Thus, in further experiments, we conducted qRT–PCR and Western blotting to detect the influence of miR-493-5p on the expression of VEGFA in ESCC. Notably, miR-493-5p overexpression decreased and miR-493-5p silencing increased the protein and mRNA levels of VEGFA (Figure 3A and B). Additionally, an ELISA confirmed that miR-493-5p also suppressed the secretion of VEGFA (Figure 3C). Bevacizumab, which can specifically inhibit the interaction between VEGFA and VEGFR2 to inhibit angiogenesis, has been used in the clinic for many cancers,[27] but its effectiveness is limited by the fact that tumors have evolved bypassing pathways to attenuate their reliance on VEGFA. Given that miR-493-5p not only suppresses ESCC cell secretion of VEGFA but also exerts intracellular effects when it is released from exosomes, we presumed that miR-493-5p might exert synergistic angiostatic effects with bevacizumab. In vivo, in a subcutaneous xenograft model, the xenograft tumor volume and tumor weight were markedly lower in the miR-493-5p-overexpressing group than in the NC group (Figure 3D–H). Consistently, the IHC results revealed decreased MVD and VEGFA staining intensity in the miR-493-5p overexpression group, indicating the angiostatic effect of miR-493-5p (Figure 3I and J). Moreover, miR-493-5p overexpression combined with bevacizumab treatment decreased xenograft tumor volume, MVD and VEGFA staining intensity to a greater extent than did bevacizumab treatment alone (Figure 3D–J), which suggested that upregulation of miR-493-5p increases the antiangiogenic effect bevacizumab in ESCC.
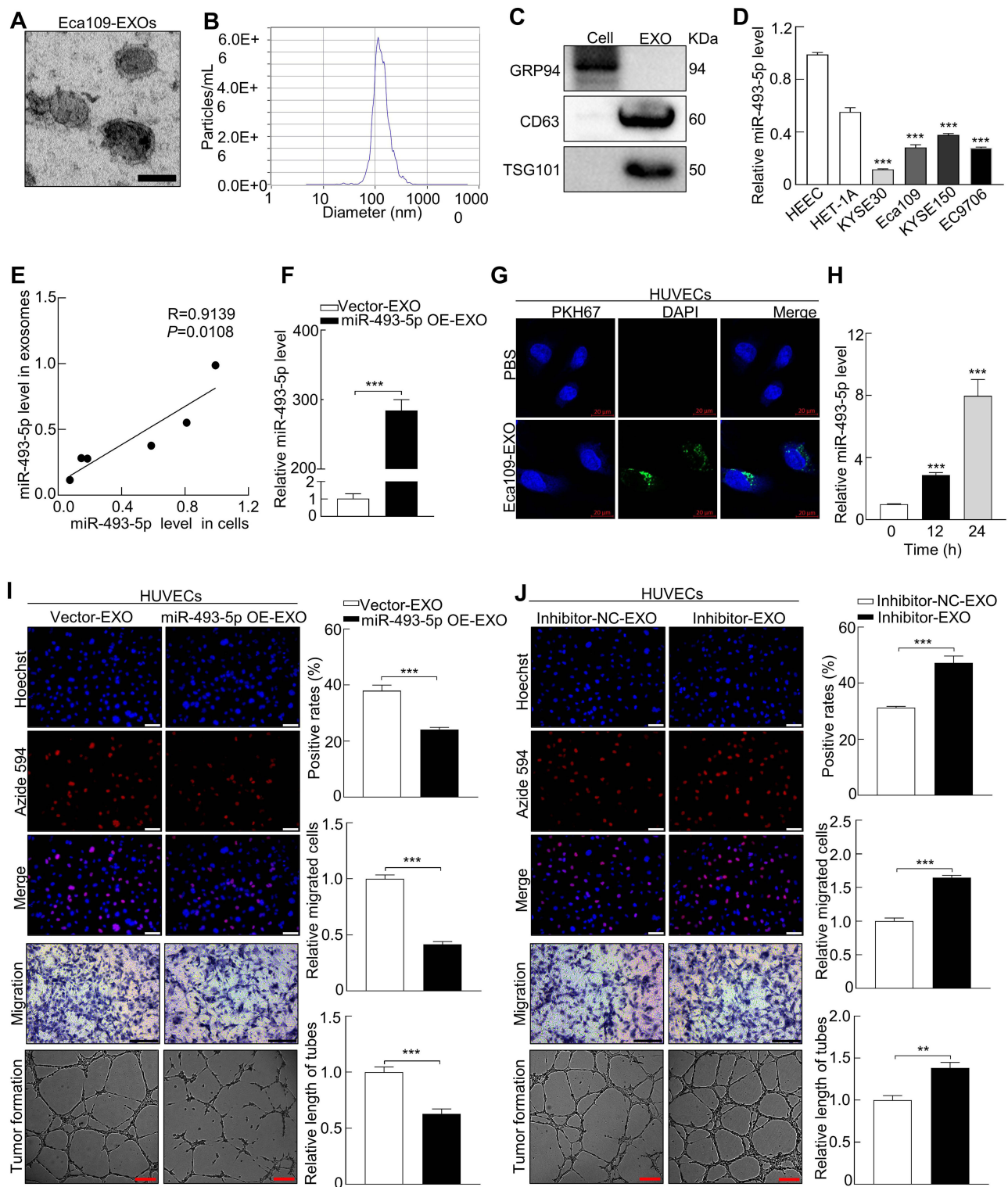
Figure 2 Exosomal miR-493-5p suppresses the cell proliferation, migration, and tube formation of HUVECs in vitro. (**A** and **B**) The morphology and size distribution of the ESCC-derived exosomes (EXO) were identified by a transmission electron microscope (scale bar=100 nm) and NanoSight tracking analysis. (**C**) Western blot analysis of CD63, TSG101, and negative marker GRP94 in exosomes. (**D**) qRT–PCR analysis of miR-493-5p expression in exosomes from 2 esophageal epithelial cell lines and 4 ESCC cell lines. (**E**) Correlation between cellular miR-493-5p expression levels and paired exosomal miR-493-5p expression levels in different cell lines. (**F**) qRT–PCR analysis of miR-493-5p expression in exosomes derived from Eca109 cells after miR-493-5p overexpression. (**G**) Labeled Eca109-EXOs (green fluorescent dye, PKH67) were taken up by HUVECs. Scale bar, 10 μm. (**H**) qRT–PCR analysis of miR-493-5p expression in HUVECs after incubation with Eca109$_{miR-493-5p\ OE}$-EXOs for 0,12 and 24 h. (**I** and **J**) The effects of exosomal miR-493-5p on proliferation, migration and tube formation ability of HUVECs detected by EdU (scale bar, 50 μm), Transwell (scale bar, 100 μm), and tube formation assays (scale bar, 100 μm). In vitro experiments were performed in triplicate, and the data are represented as the mean ± SD, **$P<0.01$, ***$P<0.001$.
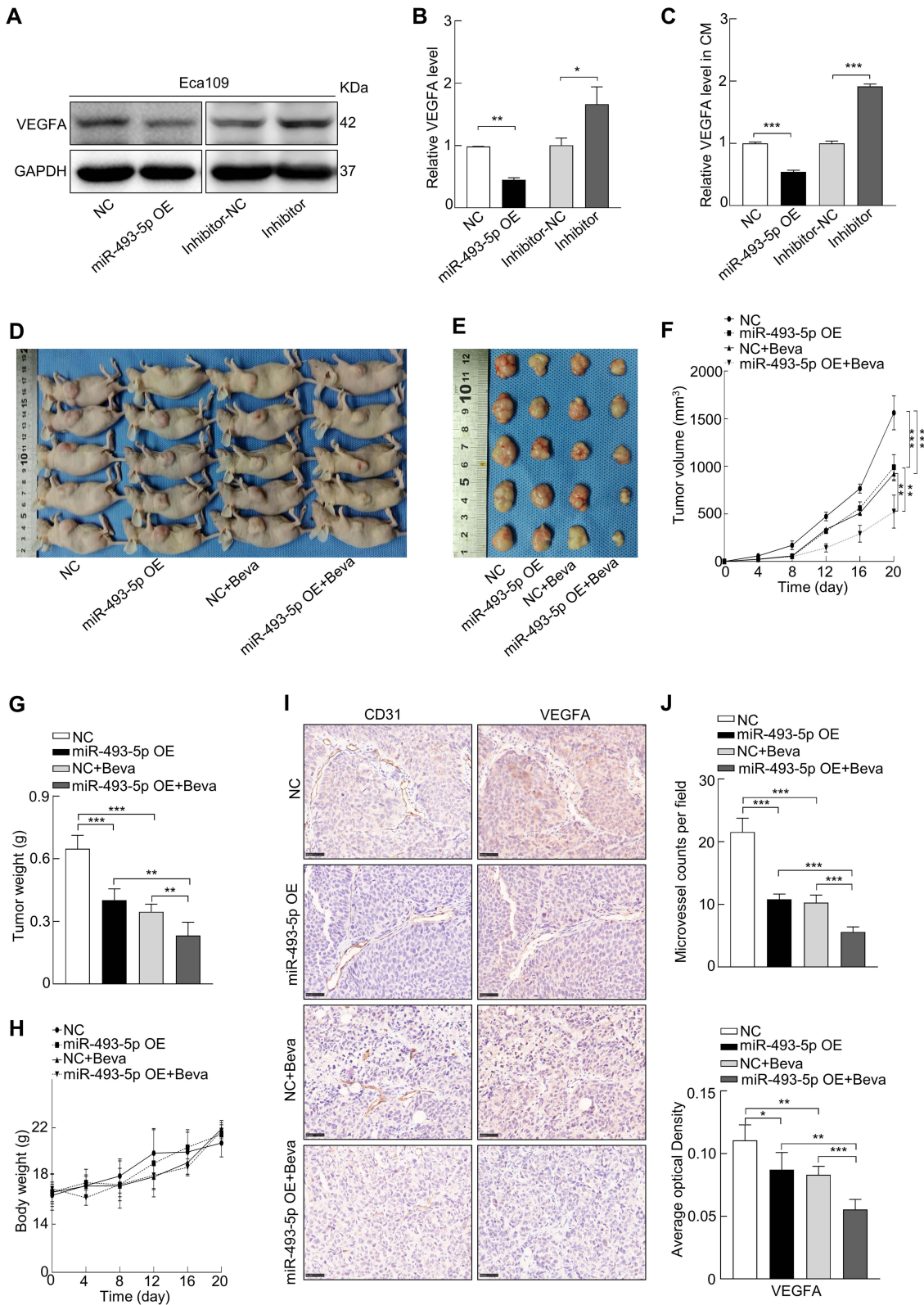
Figure 3 miR-493-5p increases the anti-tumor effect of bevacizumab via a VEGFA-dependent pathway. (**A**) Western blot analysis of VEGFA proteins in Eca109 treated with the indicated agent. (**B**) qRT–PCR analysis of the VEGFA expression in Eca109 treated with the indicated agent. (**C**) ELISA assay determined the secretion of VEGFA in the CM of Eca109 treated with the indicated agent. (**D**) Representative image of xenograft model of all groups. (**E**) Representative image of enucleated xenograft tumor of all groups. (**F–H**) Quantitative analysis of nude mice's xenograft tumor volume changing, xenograft tumor weight, and nude mice body weight changing of all groups. (**I**) Representative images of IHC staining for CD31 and VEGFA in each group (scale bar, 100 μm). (**J**) Quantitative analysis of MVD, as indicated by CD31-positive microvessels, and average optical density of VEGFA detected by IHC assay. In vitro experiments were performed in triplicate, and the data are represented as the mean ± SD, Beva, bevacizumab, *$P<0.05$, **$P<0.01$, ***$P<0.001$.

SP1 and SP3 are Direct Target Genes of miR-493-5p

miRNAs bind predominantly to the 3'-UTR of target genes to exert posttranscriptional suppression effects.[28] According to the results of GO analysis (Figure 4A and B), we identified 4 transcription factors (SP1, SP3, HIF-1α and E2F3) that are upregulated in ESCC tissues (Figure S3A) and closely related to tumor angiogenesis.[29–31] The qRT–PCR results revealed that miR-493-5p overexpression notably decreased the expression levels of SP1 and SP3 and that silencing miR-493-5p significantly increased the expression levels of SP1 and SP3 (Figure 4C and D and S3B). However, the mRNA levels of HIF-1α and E2F3 changed only when miR-493-5p was overexpressed; no difference was detected when miR-493-5p was knocked down (Figure S3B). Therefore, we chose SP1 and SP3 for further investigation. The Western blotting results showed that the SP1 and SP3 protein levels were also decreased by miR-493-5p (Figure 4E). To examine whether miR-493-5p directly binds to the 3'-UTRs of SP1 and SP3, we performed dual-luciferase reporter analysis in HEK-293T cells. The inhibitory effect of miR-493-5p on the activity of the firefly luciferase reporter was abolished when the binding sites were mutated (Figure 4F), indicating that SP1 and SP3 are direct targets of miR-493-5p. The miR-493-5p binding sites in the SP1/SP3 mRNA 3'-UTR are listed in Figure S4A and S4B. In addition, silencing of SP1 and SP3 in ESCC markedly decreased VEGFA expression (Figure S5A–S5D), which led us to speculate that SP1/SP3 is indispensable for miR-493-5p-mediated angiogenesis in ESCC. Therefore, we performed a series of rescue experiments and found that SP1/SP3 overexpression reversed the inhibitory effects of the miR-493-5p mimics on HUVECs proliferation, migration and tube formation (Figure 4G and H, Figure S6A and S6B). These results indicate that miR-493-5p exerts its angiostatic effect by directly targeting SP1 and SP3.

miR-493-5p Inhibits Angiogenesis of HUVECs via Suppressing the SP1/SP3-Activated MAPK Signaling Pathway

Accumulating evidence has shown that various signaling pathways, such as the PI3K-AKT, Wnt/β-catenin, and MAPK signaling pathways, are activated during angiogenesis.[32–34] KEGG enrichment analysis indicated that the 315 target genes were enriched in the "MAPK signaling pathway" (Figure 5A). Since MAPK cascades involve many kinases, such as MAP/ERK kinases (MEKs), ERK1/2 in the canonical MAPK pathway, and p38 MAPK in the noncanonical pathway,[35] we next explored whether miR-493-5p exerts its antiangiogenic effect through the MAPK pathway. As shown in Figure 5B, phosphorylated MEK (p-MEK), phosphorylated ERK1/2 (p-ERK1/2) and phosphorylated p38MAPK (p-p38MAPK) levels were markedly reduced after miR-493-5p overexpression and increased after administration of the miR-493-5p inhibitor. Furthermore, silencing SP1/SP3 also decreased the expression levels of p-MEK, p-ERK1/2 and p-p38MAPK in HUVECs (Figure S7A and S7B). Given these results, we investigated whether miR-493-5p regulates the MAPK pathway via the SP1/SP3 pathway via a series of rescue assays. The results revealed that re-expression of SP1/SP3 attenuated the miR-493-5p-mediated inhibition of p-MEK, p-ERK1/2 and p-p38MAPK expression in HUVECs (Figure 5C). Silencing SP1/SP3 not only attenuated the increase in p-MEK, p-ERK1/2 and p-p38MAPK expression in HUVECs induced by treatment with Eca109$_{miR-493-5p-inhibitor}$-EXOs (Figure 5D) but also reversed the promoting effects of Eca109$_{miR-493-5p-inhibitor}$-EXOs on the proliferation, migration and tube formation of HUVECs (Figure 5E–G). Collectively, these data indicated that miR-493-5p inhibits angiogenesis mediated by HUVECs through the SP1/SP3-activated MAPK signaling pathway.

Decitabine Increases the Antitumor Effect of Bevacizumab by Upregulating the Expression of miR-493-5p in ESCC

Previous studies have demonstrated that altered DNA methylation in the promoter region leads to changes in miRNA expression.[36,37] Consistent with these findings, we found that miR-493-5p expression in ESCC increased in response to treatment with decitabine in concentration - and time-dependent manners (Figure 6A and B). Decitabine is a frequently prescribed DNA methyltransferase agonist in tumor therapy.[38] Hence, we speculated that methyltransferases may be involved in this process. Theoretically, the de novo establishment of DNA methylation is regulated by the DNA methyltransferases DNMT3A and DNMT3B, whereas DNA methylation maintenance is mediated by DNMT1.[39] The qRT–PCR results revealed that DNMT3A, DNMT3B and DNMT1 downregulated the expression of miR-493-5p (Figure 6C), and miR-493-5p could be re-expressed by shDNMT3A or shDNMT3B. However, knocking down
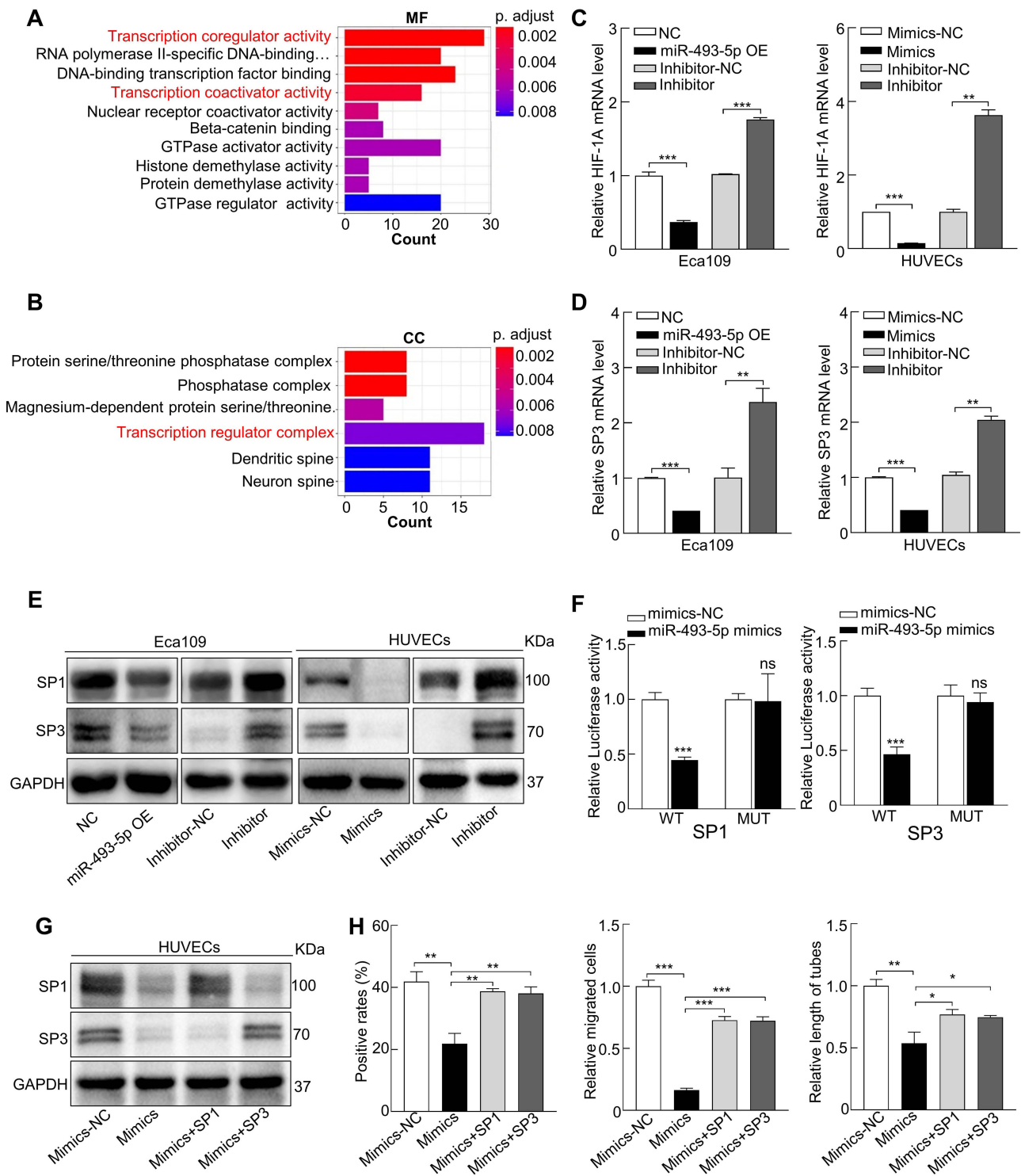
Figure 4 SP1 and SP3 are direct target genes of miR-493-5p. (**A** and **B**) GO analysis of the 315 candidate target genes. (**C** and **D**) qRT–PCR analysis of SP1 and SP3 expression in Eca109 and HUVECs treated with the indicated agent. (**E**) Western blot analysis of SP1 and SP3 proteins in Eca109 and HUVECs treated with the indicated agent. (**F**) The target relationship between miR-493-5p and SP1, SP3 was verified by dual luciferase reporter assays. (**G**) Western blot analysis of SP1 and SP3 in HUVECs treated with the indicated agent. (**H**) Quantitative analysis of the proliferation, migration, tube formation ability of HUVECs rescued by SP1 and SP3 overexpression detected by EdU, Transwell, and tube formation assays. In vitro experiments were performed in triplicate, and the data are represented as the mean ± SD, ns no significance, *P<0.05, **P<0.01, ***P<0.001.
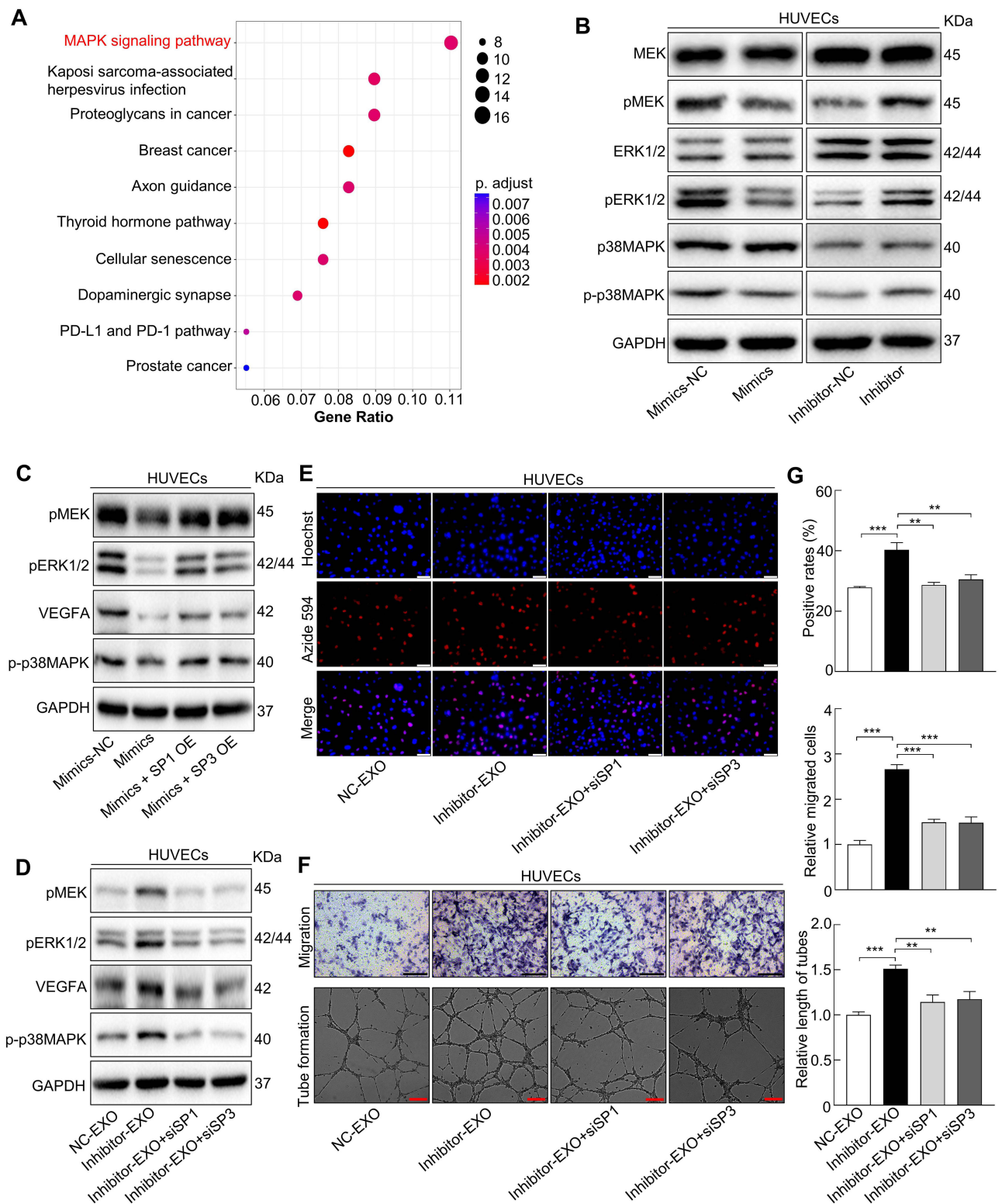**Abbreviations**: MF, molecular function; CC, cellular component.

Figure 5 miR-493-5p inhibits angiogenesis of HUVECs via suppressing the SP1/SP3-activated MAPK signaling pathway. (**A**) KEGG enrichment analysis of 315 miR-493-5p target genes. (**B–D**) Western blot analysis of MAPK-related markers in HUVECs treated with the indicated agent. (**E** and **F**) Representative images of silencing SP1 and SP3 to rescue proliferation, migration and tube formation abilities of HUVECs detected by EdU (scale bar, 50 μm), Transwell (scale bar, 100 μm) and tube formation assays (scale bar, 100 μm). (**G**) Quantitative analysis of the proliferation, migration, and tube formation abilities of HUVECs rescued by silencing SP1 and SP3 detected by EdU, Transwell, and tube formation assays. In vitro experiments were performed in triplicate, and the data are represented as the mean ± SD, **$P<0.01$, ***$P<0.001$.
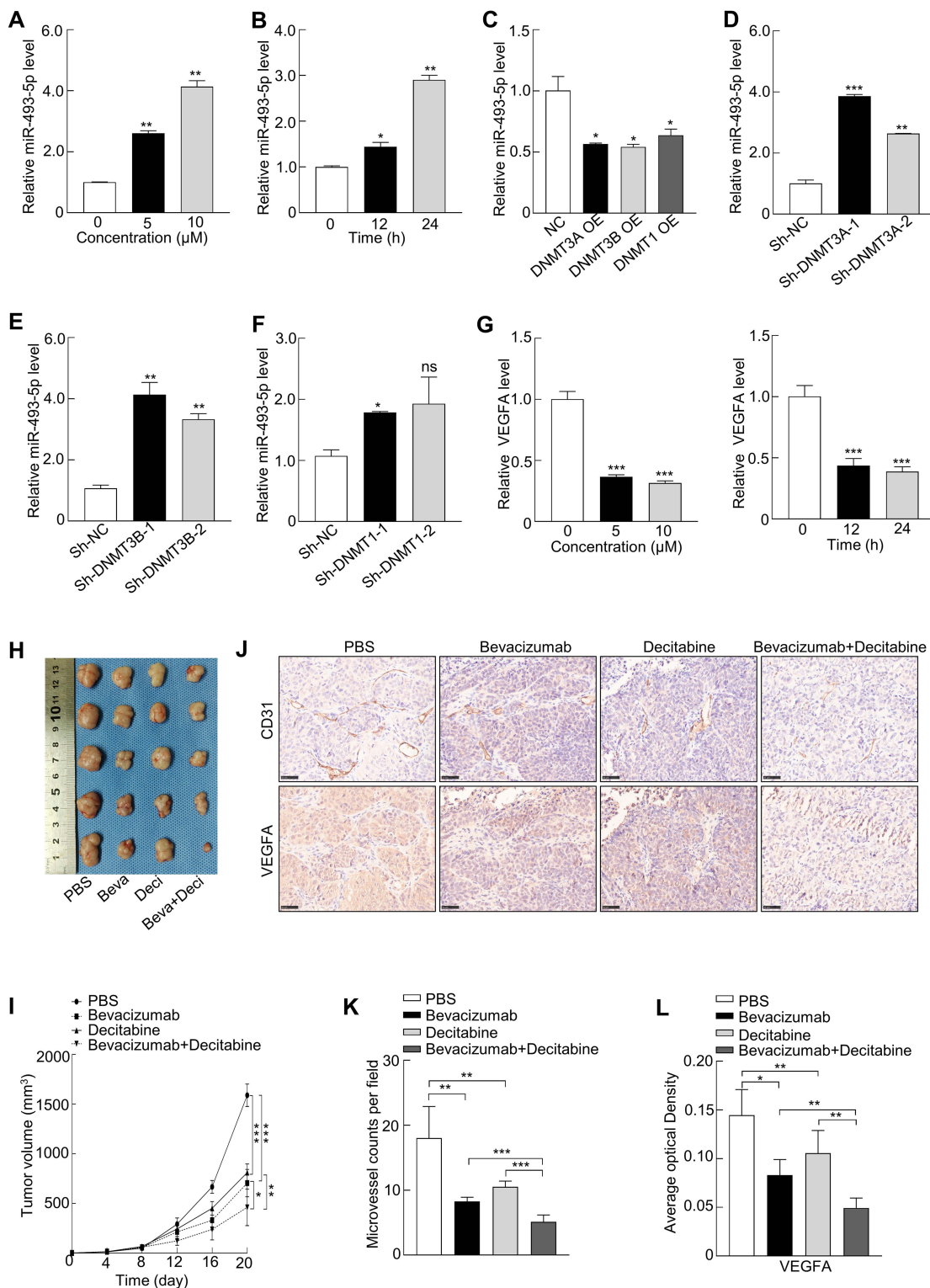
Figure 6 Decitabine increases the antitumor effect of bevacizumab by upregulating expression of miR-493-5p in ESCC. (**A**) qRT–PCR analysis of miR-493-5p expression in Eca109 cells after administration with decitabine under concentration of 0, 5, 10 μM for 24 h. (**B**) qRT–PCR analysis of miR-493-5p expression in Eca109 cells after administration with decitabine under concentration of 5 μM for 0, 12, 24 h. (**C**) qRT–PCR analysis of miR-493-5p expression in Eca109 cells after overexpression of DNMT3A, DNMT3B, DNMT1. (**D–F**) qRT–PCR analysis of miR-493-5p expression in Eca109 cells after knockdown of DNMT3A, DNMT3B, and DNMT1. (**G**) qRT–PCR analysis of VEGFA expression in Eca109 cells after administration with decitabine under concentration of 0, 5, 10 μM for 24 h (left) and under concentration of 5 μM for 0, 12, 24 h (right). (**H**) Representative image of enucleated xenograft tumor of all groups. (**I**) Quantitative analysis of nude mice's xenograft tumor volume changing of all groups. (**J**) Representative images of IHC staining for CD31 and VEGFA in each group (scale bar, 50 μm). (**K** and **L**) Quantitative analysis of MVD, as indicated by CD31-positive microvessels, and average optical density of VEGFA detected by IHC assays. In vitro experiments were performed in triplicate, and the data are represented as the mean ± SD, *$P<0.05$, **$P<0.01$, ***$P<0.001$.
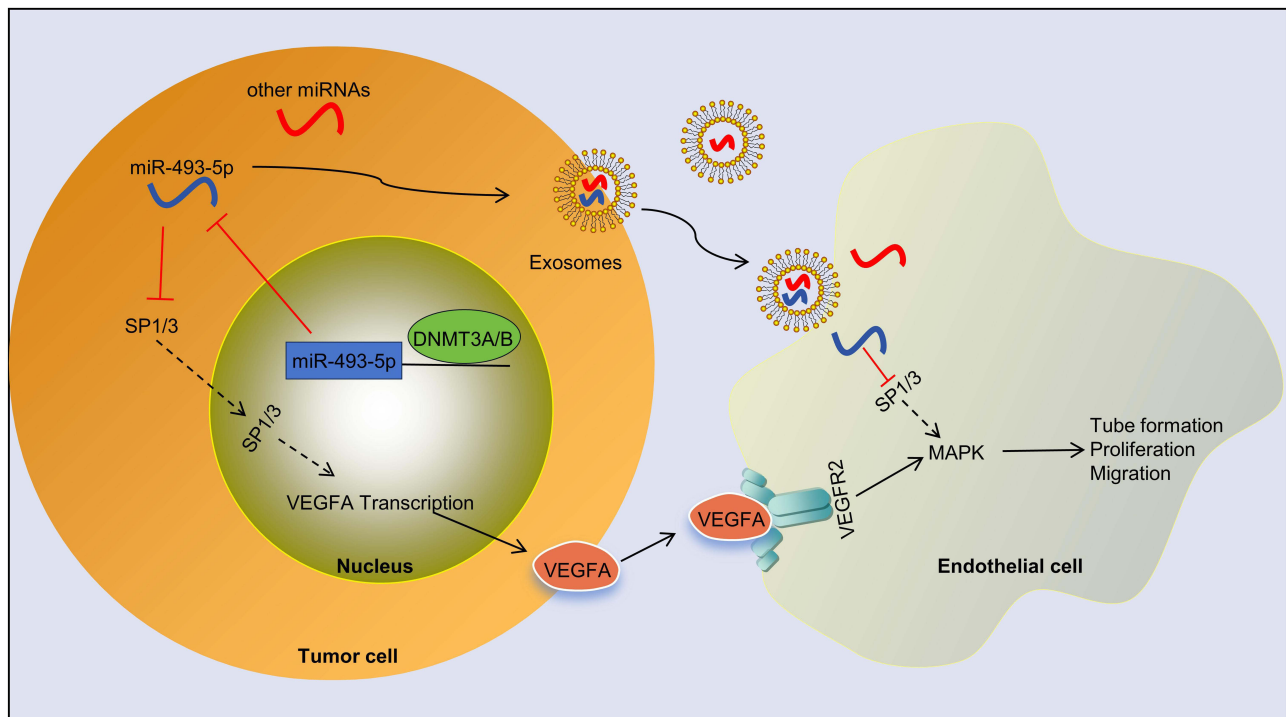**Abbreviations**: Beva, bevacizumab; Deci, decitabine; ns, no significance.

Figure 7 Schematic diagram showing that miR-493-5p suppresses the cell proliferation, migration, and tube formation of HUVECs via exosomes and a VEGFA-dependent manner.

DNMT1 had no significant effect on miR-493-5p (Figure 6D–F). Interestingly, we found that the administration of decitabine notably decreased VEGFA levels (Figure 6G), suggesting that decitabine may have promising potential for controlling ESCC angiogenesis.

Having proven that miR-493-5p overexpression increases the antiangiogenic effect of bevacizumab on ESCC, we sought to determine whether decitabine has an identical effect on bevacizumab because decitabine can restore the expression of miR-493-5p. Therefore, Eca109 cells were engrafted into nude mice to generate xenograft tumors. Strikingly, the combination of decitabine and bevacizumab reduced the xenograft tumor volume compared to that in the groups treated with decitabine or bevacizumab alone (Figures 6H, I and S8A–S8C). IHC staining of CD31 and VEGFA in tumor tissue also confirmed that the bevacizumab plus decitabine group had the lowest microvascular density (MVD) and optical density value for VEGFA (Figure 6J–L). In summary, decitabine increases the expression of miR-493-5p in ESCC by inhibiting DNMT3A/B, which increases the antiangiogenic effect of bevacizumab. A working model of our study has been summarized (Figure 7).

Discussion

In this study, we demonstrated that miR-493-5p was consistently downregulated in the plasma exosomes of ESCC patients vs those of healthy controls and had high diagnostic value for ESCC. In addition, we found that miR-493-5p, a candidate tumor suppressor, not only inhibited the proliferation, migration and tube formation of HUVECs in a VEGFA-dependent manner but also exerted its angiostatic effect via exosomes. Further investigation revealed that its angiostatic effect depends on the miR-493-5p-SP1/SP3-MAPK axis. Moreover, we found that miR-493-5p could be regulated by DNMT3A and DNMT3B, and either the overexpression of miR-493-5p or the restoration of miR-493-5p expression with decitabine could increase the antiangiogenic and antitumor effects of bevacizumab. Our study identified a new noninvasive biomarker for ESCC diagnosis and a promising therapeutic target for ESCC treatment.

Currently, imaging technologies such as esophageal barium radiography and endoscopic examination are the main tools used for ESCC screening. Nevertheless, there appear to be some limitations. For example, esophageal barium

radiography may have low sensitivity for detecting early-stage ESCC, and endoscopic examination is invasive and expensive. Recently, the use of exosomal miRNAs in liquid biopsy samples of malignant tissue has facilitated early-stage cancer diagnosis.[12,40] Compared with esophageal barium radiography and endoscopic examination, the detection of exosomal miRNAs is more convenient, more economical and less invasive. In this study, we found that exosomal miR-493-5p expression was markedly reduced in the plasma of ESCC patients vs that of healthy controls. The ROC curve indicated that this marker has high sensitivity and specificity for ESCC diagnosis. Considering that the detection of plasma exosomal miR-493-5p is noninvasive and convenient, this miRNA might serve as a competitive potential biomarker for the early screening of ESCC.

A key initial finding in the current study was the functions and mechanisms of miR-493-5p in regulating ESCC angiogenesis. According to most reports investigating exosomal miRNA-mediated tumor angiogenesis, exosomal miRNAs are released by tumor cells and subsequently taken up by vascular epithelial cells to induce further molecular cascades, which influence vessel formation capacity.[41] The proangiogenic effect of exosomal miRNA has been widely reported. Recently, several studies demonstrated that exosomal miRNAs also could serve as antiangiogenic factors, such as exosomal miR-100-5p and exosomal miR-484.[42,43] In this study, in addition to the finding of horizontal transfer of miR-493-5p from ESCC cells to HUVECs via exosomes, we also found that the overexpression of miR-493-5p could significantly inhibit VEGFA expression and secretion. Our results confirmed that in ESCC, miR-493-5p resistance to angiogenesis occurs via an exosomal mechanism and a VEGFA-dependent mechanism. These two pathways complement each other, hence conferring strong angiostatic ability to miR-493-5p. SP1/SP3 are transcription factors involved in tumor-associated metastasis and proliferation.[44] In our study, we demonstrated that the overexpression of miR-493-5p can significantly suppress the mRNA and protein expression of SP1/SP3, and the results of a dual-luciferase reporter assay verified that SP1/SP3 are direct targets of miR-493-5p. Previous reports have revealed the relationship between SP1 and ESCC angiogenesis.[45,46] However, the connection between SP3 and ESCC angiogenesis has rarely been reported. Here, we found that the overexpression of SP1/SP3 can reverse the inhibitory effect of miR-493-5p on HUVECs, and the knockdown of SP1/SP3 can reverse the promoting effects of the miR-493-5p inhibitor on HUVECs. Collectively, these results reveal that the angiostatic effect of miR-493-5p is mediated by SP1/SP3. In addition, the formation of new blood vessels relies on the stimulation of numerous signaling pathways, including the MAPK, PI3K/Akt, Wnt and JAK/STAT pathways.[47,48] In this study, we found that either overexpressing miR-493-5p or knocking down SP1/SP3 strikingly decreased p-p38MAPK and p-ERK1/2 levels in HUVECs. Moreover, the overexpression of SP1/SP3 attenuated the inhibitory effects of miR-493-5p on MAPK signaling, indicating that miR-493-5p inhibits angiogenesis of HUVECs via the SP1/SP3-mediated MAPK signaling pathway. Overall, our comprehensive study elucidated the mechanism of miR-493-5p in regulating ESCC angiogenesis.

Another important finding was related to the potential clinical value of miR-493-5p in inhibiting angiogenesis. Bevacizumab, which can specifically target VEGFA, has been approved by the FDA for application in many cancers and has achieved impressive results.[49,50] However, some factors limit the clinical efficacy of bevacizumab. Heterogeneity among tumor patients can lead to low sensitivity or even drug resistance in some cases, even in patients with high levels of VEGFA.[51] Therefore, the identification of methods to classify tumor patients according to sensitivity to bevacizumab alone or combined with antiangiogenic agents is important for the ESCC treatment. In our in vivo experiment, miR-493-5p OE transduction and bevacizumab treatment synergistically and significantly decreased the tumor volume, indicating that miR-493-5p can strengthen the antitumor effect of bevacizumab. Further experiments demonstrated that miR-493-5p can be silenced by DNMT3A and DNMT3B. Additionally, decitabine not only restored miR-493-5p expression but also decreased the expression level of VEGFA, which suggested that decitabine may increase the antiangiogenic effects of bevacizumab. To verify the above assumption, we performed an in vivo experiment, and the data confirmed that the combination of bevacizumab and decitabine significantly decreased the xenograft tumor volume compared with that in the groups treated with bevacizumab or decitabine alone. Thus, this study highlights a novel promising therapeutic strategy for ESCC treatment.

Conclusion

In conclusion, we found that miR-493-5p expression was notably reduced in the plasma exosomes of ESCC patients vs that of healthy controls and that plasma exosomal miR-493-5p might serve as a noninvasive biomarker for ESCC screening. miR-493-5p not only inhibited the proliferation, migration and tube formation of HUVECs in a VEGFA-dependent manner

but also exerted an angiostatic effect via exosomes. Overexpression of miR-493-5p or restoration of miR-493-5p expression with decitabine increased the antitumor effects of bevacizumab, which highlights a promising therapeutic strategy for ESCC treatment.

Abbreviations

miRNAs, microRNAs; ESCC, esophageal squamous cell carcinoma; FDA, Food and Drug Administration; TEM, transmission electron microscopy; NTA, NanoSight tracking analysis; GEO, Gene Expression Omnibus; ROC, receiver operating characteristic; HUVECs, human umbilical vein endothelial cells; DNMT3A/3B, DNA methyltransferase 3A/3B; VEGF, vascular endothelial growth factors; CM, culture medium; OD, optical density; MVD, micro-vessel density; EXOs, exosomes; p-MEK, phosphorylated MEK; p-ERK1/2, phosphorylated ERK1/2; p-p38MAPK, phosphorylated p38MAPK; Eca109$_{\text{miR-493-5p-OE}}$-EXOs, exosomes extracted from miR-493-5p overexpressed Eca109 cells; Eca109$_{\text{miR-493-5p-inhibitor}}$-EXOs, exosomes extracted from Eca109 cells transfected with miR-493-5p inhibitors.

Data Sharing Statement

The publicly available data are provided in the GEO database. And all the other data supporting this study are available within this article, Supplementary Materials, as well as source data. Source data are provided with this paper.

Ethics Statement

The study was conducted according to the principles expressed in the Declaration of Helsinki. Informed consent was obtained from all participants for obtaining clinical samples, and the ethics approval was provided by the Ethics Committee of the Second Hospital of Shandong University (protocol code: KYLL-2020(LW)-082). All the animal experiments were approved by the Second Hospital of Shandong University Animal Care Commission (protocol code: KYLL-2023(LW)-107) and performed according to the National Institutes of Health's Guide for the Care and Use of Laboratory Animals.

Acknowledgments

The authors expressed their gratitude to all members participated in this study.

Funding

Disclosure

The authors report no conflicts of interest in this work.

References

1. Eileen M, Isabelle S, Harriet R, et al. The Global Landscape of Esophageal Squamous Cell Carcinoma and Esophageal Adenocarcinoma Incidence and Mortality in 2020 and Projections to 2040: new Estimates From GLOBOCAN 2020. *Gastroenterology.* 2022;163(3):649–658.
2. Thrift A. Global burden and epidemiology of Barrett oesophagus and oesophageal cancer. *Nat Rev Gastroenterol Hepatol.* 2021;18(6):432–443. doi:10.1038/s41575-021-00419-3
3. Mahdi S, Gholamreza R, Valerie M, et al. Current Status and Future Prospects for Esophageal Cancer. *Cancers (Basel).* 2023;15(3): 765.
4. Codipilly D, Qin Y, Dawsey S, et al. Screening for esophageal squamous cell carcinoma: recent advances. *Gastrointest Endosc.* 2018;88(3):413–426. doi:10.1016/j.gie.2018.04.2352
5. Yan-Ming Y, Pan H, Wen Wen X, et al. Advances in targeted therapy for esophageal cancer. *Signal Transduct Target Ther.* 2020;5(1): 229.
6. Subhash BA, Samuel PC, Carole AP. The ins-and-outs of exosome biogenesis, secretion, and internalization. *Trends Cell Biol.* 2023;34(2):229.
7. Liu J, Ren L, Li S, et al. The biology, function, and applications of exosomes in cancer. *Acta pharmaceutica Sinica B.* 2021;11(9):2783–2797. doi:10.1016/j.apsb.2021.01.001
8. Mohammadi M, Zargartalebi H, Salahandish R, et al. Emerging technologies and commercial products in exosome-based cancer diagnosis and prognosis. *Biosens. Bioelectron.* 2021;183:113176.

9. Preethi K, Selvakumar S, Ross K, et al. Liquid biopsy: exosomal microRNAs as novel diagnostic and prognostic biomarkers in cancer. *Mol Cancer*. 2022;21(1):54. doi:10.1186/s12943-022-01525-9

10. Arcucci V, Stacker S, Achen M. Control of gene expression by exosome-derived non-coding RNAs in cancer angiogenesis and lymphangiogenesis. *Biomolecules*. 2021;11(2):249. doi:10.3390/biom11020249

11. Yang X, Zhang Y, Zhang Y, et al. The key role of exosomes on the pre-metastatic niche formation in tumors. *Front Mol Biosci*. 2021;8:703640. doi:10.3389/fmolb.2021.703640

12. Lijun Z, Lili Y, Xiangpeng W, et al. Mechanisms of function and clinical potential of exosomes in esophageal squamous cell carcinoma. *Cancer Lett*. 2022;553:215993.

13. Liwen H, Kai X, Chao Z, et al. Exosomal MALAT1 promotes the proliferation of esophageal squamous cell carcinoma through glyoxalase 1-dependent methylglyoxal removal. *Noncoding RNA Res*. 2024;9(2): 330–40.

14. Viallard C, Larrivée B. Tumor angiogenesis and vascular normalization: alternative therapeutic targets. *Angiogenesis*. 2017;20(4):409–426. doi:10.1007/s10456-017-9562-9

15. Pérez-Gutiérrez L, Ferrara N. Biology and therapeutic targeting of vascular endothelial growth factor A. *Nat Rev Mol Cell Biol*. 2023;24 (11):816–834. doi:10.1038/s41580-023-00631-w

16. Ellis L, Kirkpatrick P. Bevacizumab nature reviews. *Drug Discovery*. 2005;4(5):S8–9. doi:10.1038/nrd1727

17. Cao Y, Langer R, Ferrara N. Targeting angiogenesis in oncology, ophthalmology and beyond. *Nat Rev Drug Discov*. 2023;22(6):476–495. doi:10.1038/s41573-023-00671-z

18. Usui-Ouchi A, Friedlander M. Anti-VEGF therapy: higher potency and long-lasting antagonism are not necessarily better. *J Clin Invest*. 2019;129 (8):3032–3034. doi:10.1172/JCI129862

19. Tian X, Liu Y, Wang Z, et al. miR-144 delivered by nasopharyngeal carcinoma-derived EVs stimulates angiogenesis through the FBXW7/ HIF-1alpha/VEGF-A axis. *Mol Ther Nucleic Acids*. 2021;24:1000–1011. doi:10.1016/j.omtn.2021.03.016

20. Rui-Min C, Yao F, Jun Z, et al. Cancer-derived exosomal miR-197-3p confers angiogenesis via targeting TIMP2/3 in lung adenocarcinoma metastasis. *Cell Death Dis*. 2022;13(12): 1032.

21. Quan Y, Jing L, Yiding L, et al. Tumor-associated macrophage-derived exosomal miR21-5p promotes tumor angiogenesis by regulating YAP1/HIF-1α axis in head and neck squamous cell carcinoma. *Cell Mol Life Sci*. 2024;81(1): 1–23.

22. Xiao Z, Feng X, Zhou Y, et al. Exosomal miR-10527-5p inhibits migration, invasion, lymphangiogenesis and lymphatic metastasis by affecting Wnt/β-catenin signaling via Rab10 in esophageal squamous cell carcinoma. *Int j Nanomed*. 2023;18:95–114. doi:10.2147/IJN.S391173

23. Liu H, Li Z, Sun H. MiR-493-5p inhibits the malignant development of gliomas via suppressing E2F3-mediated dysfunctions of P53 and PI3K/ AKT pathways. *Clin Trans Oncol: Official Publication of the Federation of Spanish Oncology Societies and of the National Cancer Institute of Mexico*. 2022;24(2):363–370. doi:10.1007/s12094-021-02698-3

24. Wang A, Chen Y, Shi L, et al. Tumor-suppressive MEG3 induces microRNA-493-5p expression to reduce arabinocytosine chemoresistance of acute myeloid leukemia cells by downregulating the METTL3/MYC axis. *J Transl Med*. 2022;20(1):288. doi:10.1186/s12967-022-03456-x

25. Yasukawa K, Liew L, Hagiwara K, et al. MicroRNA-493-5p-mediated repression of the MYCN oncogene inhibits hepatic cancer cell growth and invasion. *Cancer Sci*. 2020;111(3):869–880. doi:10.1111/cas.14292

26. Chen S, Chen X, Luo Q, et al. Retinoblastoma cell-derived exosomes promote angiogenesis of human vesicle endothelial cells through microRNA-92a-3p. *Cell Death Dis*. 2021;12(7):695. doi:10.1038/s41419-021-03986-0

27. Garcia J, Hurwitz H, Sandler A, et al. Bevacizumab (Avastin®) in cancer treatment: a review of 15 years of clinical experience and future outlook. *Cancer Treat Rev*. 2020;86:102017. doi:10.1016/j.ctrv.2020.102017

28. Shang R, Lee S, Senavirathne G, et al. microRNAs in action: biogenesis, function and regulation. *Nat Rev Genet*. 2023;24(12):816–833. doi:10.1038/s41576-023-00611-y

29. Lu H, Yuan P, Ma X, et al. Angiotensin-converting enzyme inhibitor promotes angiogenesis through Sp1/Sp3-mediated inhibition of notch signaling in male mice. *Nat Commun*. 2023;14(1):731. doi:10.1038/s41467-023-36409-z

30. Palazon A, Tyrakis P, Macias D, et al. An HIF-1α/VEGF-A axis in cytotoxic T cells regulates tumor progression. *Cancer Cell*. 2017;32(5):669–683. e665. doi:10.1016/j.ccell.2017.10.003

31. Zhou J, Cheng M, Wu M, et al. Contrasting roles of E2F2 and E2F3 in endothelial cell growth and ischemic angiogenesis. *J Mol Cell Cardiol*. 2013;60:68–71. doi:10.1016/j.yjmcc.2013.04.009

32. Fang H, Sun Q, Zhou J, et al. mA methylation reader IGF2BP2 activates endothelial cells to promote angiogenesis and metastasis of lung adenocarcinoma. *Mol Cancer*. 2023;22(1):99. doi:10.1186/s12943-023-01791-1

33. Lv F, Li X, Wang Y, et al. MAGP1 maintains tumorigenicity and angiogenesis of laryngeal cancer by activating Wnt/β-catenin/MMP7 pathway. *Carcinogenesis*. 2024;45(4):220–234. doi:10.1093/carcin/bgad003

34. Zink J, Frye M, Frömel T, et al. EVL regulates VEGF receptor-2 internalization and signaling in developmental angiogenesis. *EMBO Rep*. 2021;22 (2):e48961. doi:10.15252/embr.201948961

35. Martin-Vega A, Cobb M. Navigating the ERK1/2 MAPK Cascade. *Biomolecules*. 2023;13(10): 155. doi:10.3390/biom13101555

36. Zhu B, Chen J, Feng Y, et al. DNMT1-induced miR-378a-3p silencing promotes angiogenesis via the NF-κB signaling pathway by targeting TRAF1 in hepatocellular carcinoma. *J Exp Clin Cancer Res*. 2021;40(1):352. doi:10.1186/s13046-021-02110-6

37. Liang L, Cen H, Huang J, et al. The reversion of DNA methylation-induced miRNA silence via biomimetic nanoparticles-mediated gene delivery for efficient lung adenocarcinoma therapy. *Mol Cancer*. 2022;21(1):186. doi:10.1186/s12943-022-01651-4

38. Zhou Z, Li HQ, Liu F. DNA methyltransferase inhibitors and their therapeutic potential. *Curr. Top. Med. Chem*. 2018;18(28):2448–2457. doi:10.2174/1568026619666181120150122

39. Chen Z, Zhang Y. Role of mammalian DNA methyltransferases in development. *Annu. Rev. Biochem*. 2020;89(1):135–158. doi:10.1146/annurev-biochem-103019-102815

40. Shin H, Choi B, Shim O, et al. Single test-based diagnosis of multiple cancer types using Exosome-SERS-AI for early stage cancers. *Nat Commun*. 2023;14(1):1644. doi:10.1038/s41467-023-37403-1

41. Zijian M, Ke W, Fengming Y, et al. Tumor-derived exosomal miR-3157-3p promotes angiogenesis, vascular permeability and metastasis by targeting TIMP/KLF2 in non-small cell lung cancer. *Cell Death Dis*. 2021;12(9): 840.

42. Wu Y, Weiwen Z, Yunfei Y, et al. Exosomal miR-100-5p inhibits osteogenesis of hBMSCs and angiogenesis of HUVECs by suppressing the BMPR2/Smad1/5/9 signalling pathway. *Stem Cell Res Ther.* 2021;12(1): 1–6.

43. Zongxia Z, Ting S, Yan G, et al. Targeted delivery of exosomal miR-484 reprograms tumor vasculature for chemotherapy sensitization. *Cancer Lett.* 2022;530:45–58.

44. Wang C, Zhang S, Ma B, et al. TP53 mutations upregulate RCP expression via Sp1/3 to drive lung cancer progression. *Oncogene.* 2022;41 (16):2357–2371. doi:10.1038/s41388-022-02260-7

45. Lin C, Song L, Liu A, et al. Overexpression of AKIP1 promotes angiogenesis and lymphangiogenesis in human esophageal squamous cell carcinoma. *Oncogene.* 2015;34(3):384–393. doi:10.1038/onc.2013.559

46. Zhang Y, Chen C, Liu Z, et al. PABPC1-induced stabilization of IFI27 mRNA promotes angiogenesis and malignant progression in esophageal squamous cell carcinoma through exosomal miRNA-21-5p. *J Exp Clin Cancer Res.* 2022;41(1):111. doi:10.1186/s13046-022-02339-9

47. Dudley A, Griffioen A. Pathological angiogenesis: mechanisms and therapeutic strategies. *Angiogenesis.* 2023;26(3):313–347. doi:10.1007/s10456-023-09876-7

48. Liu Z, Chen H, Zheng L, et al. Angiogenic signaling pathways and anti-angiogenic therapy for cancer. *Signal Transduct and Targeted Ther.* 2023;8 (1):198. doi:10.1038/s41392-023-01460-1

49. Voelker R. FDA approves first biosimilar to treat cancer. *Cancer Discovery.* 2017;7(11):1206. doi:10.1158/2159-8290.CD-NB2017-139

50. Henry FS, Michael DP, Patrick YW, et al. Bevacizumab alone and in combination with irinotecan in recurrent glioblastoma. *J Clin Oncol.* 2023;41 (32): 4945–4952.

51. Yoshiro I, Kenji K, Takamasa Y, et al. Resistance to anti-angiogenic therapy in cancer-alterations to anti-VEGF pathway. *Int J Mol Sci.* 2018;19(4): 1232.